Bifurcation to polarization self-modulation in vertical-cavity surface-emitting lasers

M. Sciamanna, F. Rogister, O. Deparis, P. Mégret, and M. Blondel

Service d'Electromagnétisme et de Télécommunications, Faculté Polytechnique de Mons, Boulevard Dolez 31, B-7000 Mons, Belgium

T. Erneux

Optique Nonlinéaire Théorique, Université Libre de Bruxelles, Campus Plaine C.P. 231, B-1050 Bruxelles, Belgium

Received September 27, 2001

Experiments have yielded polarization self-modulation in vertical-cavity surface-emitting lasers (VCSELs) subject to a $\pi/2$ polarization-rotating optical feedback. The phenomenon has been simulated numerically, but its bifurcation has never been explained. We show that polarization self-modulation results from a Hopf bifurcation mechanism that can be analyzed in terms of the laser feedback parameters. Our analysis predicts other bifurcations for low values of the feedback rate, which explain why more-complex time-dependent outputs have been observed as alternatives to polarization self-modulation. © 2002 Optical Society of America

OCIS codes: 190.3100, 250.7260.

In general, the light emitted by a cylindrical vertical-cavity surface-emitting laser (VCSEL) is linearly polarized along one of two preferential directions (called x and y).[1] Polarization self-modulation (PSM) has been experimentally observed in a VCSEL that was subjected to optical feedback through a quarter-wave plate whose optical axis was located at 45° to the VCSEL eigenaxes.[2–6] Every round-trip time, the quarter-wave plate caused the polarization of the light reentering the laser cavity to rotate 90°. By a polarization injection-locking mechanism,[2] the light was then forced to switch periodically between x and y linear polarizations with a period close to twice the external cavity round-trip time. Previous numerical studies have simulated PSM,[4,5,7] but the dynamic instability that is responsible for PSM has not been elucidated.

Here we investigate the bifurcation mechanism that leads to PSM and show that more-complex forms of polarization dynamics are possible. They explain why chaotic outputs are sometimes observed,[4,5] and they agree with observations reported for TE–TM PSM experiments that used edge-emitting lasers.[8,9] Our numerical simulations use rate equations that extend those proposed by Chen and Liu[10] for TE–TM polarization bistability in edge-emitting lasers. With the external optical feedback through a quarter-wave plate taken into account, our dimensionless equations[11] are given by

$$\frac{dE_x}{ds} = \frac{1}{2}(1+i\alpha)[(1+2Z)F_x - 1]E_x + \eta E_y(s-\theta)\exp(-i\phi_f), \quad (1)$$

$$\frac{dE_x}{ds} = \frac{1}{2}(1+i\alpha)[(1+2Z)F_x - 1]E_x + \eta E_x(s-\theta)\exp(-i\phi_f), \quad (2)$$

$$T\frac{dZ}{ds} = P - Z - (1+2Z)(F_x|E_x|^2 + F_y|E_y|^2), \quad (3)$$

where

$$F_x = 1 - \epsilon_{xx}\left(|E_x|^2 - \frac{P}{2}\right) - \epsilon_{xy}\left(|E_y|^2 - \frac{P}{2}\right), \quad (4)$$

$$F_y = 1 - \epsilon_{yx}\left(|E_x|^2 - \frac{P}{2}\right) - \epsilon_{yy}\left(|E_y|^2 - \frac{P}{2}\right). \quad (5)$$

In Eqs. (1)–(5), E_x and E_y are the slowly varying linearly polarized components of the optical field, Z is the carrier density, s is time measured in units of photon lifetime, α is the linewidth enhancement factor, and $T \equiv \tau_s/\tau_p$ is the ratio of carrier lifetime τ_s to photon lifetime τ_p. η is the feedback rate normalized by ${\tau_p}^{-1}$. θ is the round-trip time in the external cavity τ divided by τ_p. $\tau \equiv 2L/c$, where L is the external cavity length and c is the speed of light. ϕ_f is the feedback phase. P is the pump parameter above threshold. Finally, F_x and F_y are two gain compression functions, where ϵ_{xx} and ϵ_{yy} represent the self-compression coefficients and ϵ_{xy} and ϵ_{yx} denote the cross-compression coefficients. Typical values of the parameters are given by[5] $P = 0.4$, $T = 1000$, $\alpha = 3$, $\epsilon_{xx} = \epsilon_{yy} = 0.02$, and $\epsilon_{xy} = \epsilon_{yx} = 0.04$. The case of a short external cavity is considered first. If $L = 1.5$ cm, $\tau_p = 1$ ps and $\tau = 100$ ps, $\theta = 100$. For simplicity, we assume that $\phi_f = 0$, and η is our control or bifurcation parameter.

Figure 1 shows a bifurcation diagram of the extrema of the x linearly polarized mode intensity $I_x \equiv |E_x|^2$ versus feedback rate η. As η is progressively increased, the laser exhibits a cascade of bifurcations between steady and periodic states. Arrows labeled a–f refer to particular dynamic states that we now describe.

As soon as η is increased from zero, we note two distinct branches of steady states (labeled a) that

0146-9592/02/040261-03$15.00/0

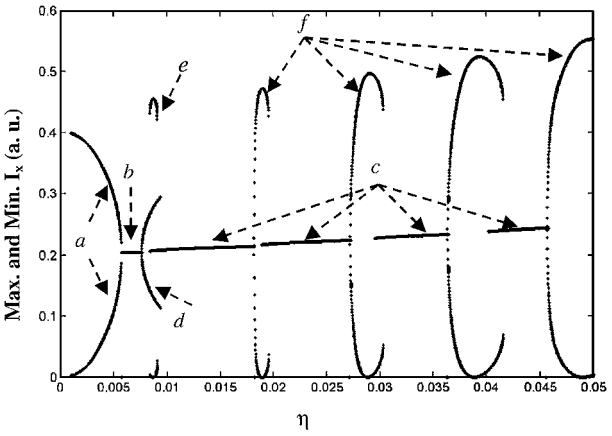

Fig. 1. Bifurcation diagram of the extrema of I_x versus η. The delay is $\theta = 100$, and the other parameters are specified in the text. The labels indicate specific dynamic states that are described in the text.

exhibit emission of both x and y linearly polarized components with $I_x \neq I_y$. The first steady state (I_y) corresponds to I_x following the upper (lower) branch. The second corresponds to I_x (I_y) following the lower (upper) branch. Because the phase difference δ between the x and y components of the field is different from a multiple of π, these steady states are elliptically polarized steady states (EPSS). The EPSS change stability to an equal-intensity steady state $I_x = I_y$ (labeled b) through a pitchfork bifurcation point. This equal-intensity steady state is an external cavity mode (ECM), as for conventional isotropic optical feedback in edge-emitting lasers.[12] More precisely, two combs of ECMs are possible for our VCSEL. They are related to a linearly polarized light aligned with one of the two eigenaxes of the compound cavity, as has been experimentally[4,6] observed. We call these two combs LK and anti-LK ECMs, respectively, depending on the phase difference δ between the x and y components: $\delta = 0$ for the LK ECMs and $\delta = \pi$ for the anti-LK ECMs. As we further increase η, LK and anti-LK ECMs (c) alternately appear. It is worthwhile to stress that no more branches of EPSS are observed. It can be shown analytically from the steady-state equations that EPSS are possible only near $\eta = 0$ and that the size of their domain in η is proportional to the magnitude of the gain compression coefficients.

Branches of time-periodic solutions emerge from Hopf bifurcations located on all the ECMs. The first branch of periodic solutions (d) corresponds to oscillations of I_x and I_y in phase [$I_x(s) = I_y(s)$; not shown]. This periodic state coexits with an isolated branch of periodic solutions (e) that exhibit antiphase oscillations in the x and y polarization modes (not shown). All the Hopf bifurcation branches that appear for $\eta > 0.018$ (f) lead to antiphase oscillations of I_x and I_y with a period close to twice the external-cavity round-trip time; see Fig. 2. These antiphase oscillations correspond to the PSM time traces observed experimentally.[2,4–6] Thus PSM is the result of a Hopf bifurcation mechanism from either an LK or an anti-LK ECM. In Fig. 1 (f), branches of periodic solutions that correspond to PSM always overlap nearby LK and anti-LK ECMs. This suggests that it is the interaction between these modes that is responsible for the PSM bifurcation phenomenon. The bifurcation can be studied both analytically and numerically, and we may identify the roles of key parameters such as pump and delay.

The bifurcation diagram of Fig. 1 corresponds to a normalized delay $\theta = 100$. However, increasing θ has dramatic effects on the bifurcation diagram. Figure 3 represents a bifurcation diagram of the steady and periodic solutions for $\theta = 140$. We first note that the EPSS admit of a Hopf bifurcation (labeled g) and a secondary torus bifurcation (h). The Hopf bifurcation leads to a periodic modulation of the EPSS, with the two polarized modes evolving in phase at a frequency close to relaxation oscillation frequency f_{RO} of the solitary VCSEL ($f_{RO} \equiv 1/2\,\pi\sqrt{2P/T} \sim 222$); see Fig. 4(a). The torus bifurcation leads to quasi-periodic oscillations; see Fig. 4(b). The two polarization intensities oscillate in phase at a high frequency close to f_{RO}, but their envelopes are partially in antiphase. Apart from these two new dynamic states observed at low feedback rates, we still find an in-phase periodic state in the x and y modes (labeled i) that coexists with an isolated branch of periodic states exhibiting an antiphase behavior (labeled j).

We next concentrate on the Hopf bifurcations to antiphase periodic oscillations that appear alternately from an LK and an anti-LK ECMs. Comparing Fig. 3 with Fig. 1, we note that all these bifurcations moved to lower values of η as we increased θ. Furthermore, Hopf bifurcation points fuse together for moderate to high feedback rates, producing a larger branch of periodic solutions (k). This means that the longer the external cavity is, the smaller is the feedback rate needed

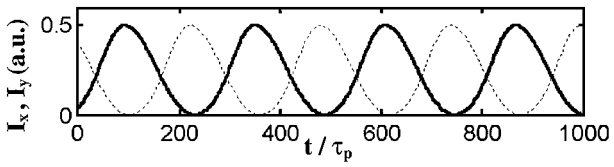

Fig. 2. Time traces of I_x and I_y for $\eta = 0.04$. The values of the other parameters are as in Fig. 1.

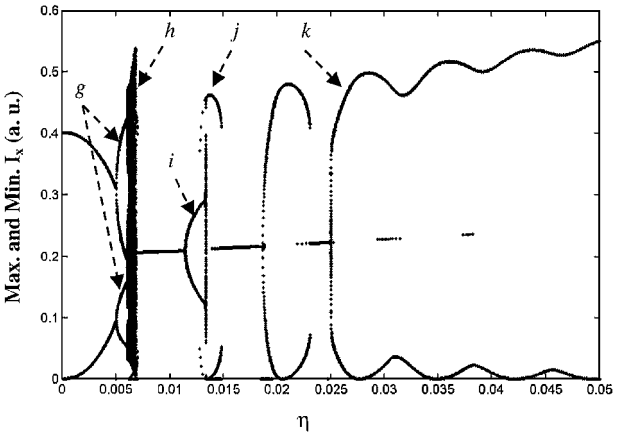

Fig. 3. Same as in Fig. 1 but for $\theta = 140$.

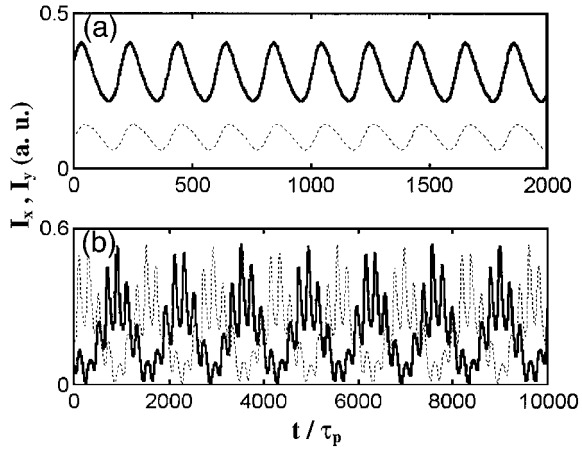

Fig. 4. (a), (b) Time traces of I_x and I_y for $\eta = 0.00564$ and $\eta = 0.0068$, respectively. The values of the other parameters are as in Fig. 3.

for stable polarization self-modulation to be observed, as was reported experimentally.[5]

In summary, we have shown that experimentally observed PSM in VCSELs subject to $\pi/2$ polarization-rotating optical feedback results from a Hopf bifurcation to antiphase periodic oscillations from either an LK or an anti-LK ECM (labeled f in Fig. 1). A minimum feedback rate is needed for observation of PSM, and increasing the delay leads to a continuous domain of antiphase oscillations for sufficiently large values of the feedback rate. Other regimes such as elliptically polarized steady states, coexisting antiphase and in-phase periodic states, and quasi-periodic states are possible but occur only for relatively low values of the feedback rate and depend strongly on the gain compression coefficients. From our numerical simulations we also noted that the compression coefficients have a stabilizing effect for the large branch of periodic solutions shown by k in Fig. 3. The PSM phenomenon described in this Letter persists as the result of a Hopf bifurcation as we change the values of the parameters. The bifurcation transition to PSM is also observed if we consider the effect of coupling between spin sublevels[4,13] in the VCSEL dynamics. This result suggests that PSM is the consequence of an injected and delayed polarized field rather than of the complex physical nature of the VCSEL device. Our results have provided motivation for future experimental studies at low feedback rates as well as observations of PSM for fixed values of the feedback rate but different external cavities. Finally, the interaction and fusion of Hopf bifurcation points seen in Fig. 3 play important roles in the stability of the PSM regimes and have provided motivation for future detailed studies of the Hopf bifurcation branches.

The authors acknowledge support from the Fonds National de la Recherche Scientifique (Belgium) and the IAP IV-07 project of the Belgian government. The research of T. Erneux is also supported by U.S. Air Force Office of Scientific Research grant AFOSR F49620-98-1-0400 and National Science Foundation grant DMS-9973203. M. Sciamanna's e-mail address is sciamanna@telecom.fpms.ac.be.

References

1. A. K. Jansen van Doorn, M. P. Van Exter, and J. P. Woerdman, Appl. Phys. Lett. **69,** 1041 (1996).
2. S. Jiang, Z. Pan, M. Dagenais, R. A. Morgan, and K. Kojima, Appl. Phys. Lett. **63,** 3545 (1993).
3. N. Badr, I. H. White, M. R. T. Tan, Y. M. Young, and S. Y. Wang, Electron. Lett. **30,** 1227 (1994).
4. F. Robert, P. Besnard, M. L. Chares, and G. M. Stephan, IEEE J. Quantum Electron. **33,** 2231 (1997).
5. H. Li, A. Hohl, A. Gavrielides, H. Hou, and K. D. Choquette, Appl. Phys. Lett. **72,** 2355 (1998).
6. G. Ropars, P. Langot, M. Brunel, M. Vallet, F. Bretenaker, A. Le Floch, and K. D. Choquette, Appl. Phys. Lett. **70,** 2661 (1997).
7. C. Masoller and N. B. Abraham, Appl. Phys. Lett. **74,** 1078 (1999).
8. W. H. Loh, Y. Ozeki, and C. L. Tang, Appl. Phys. Lett. **56,** 2613 (1990).
9. C. L. Tang, J. Opt. B **10,** R51 (1998).
10. Y. C. Chen and J. M. Liu, Appl. Phys. Lett. **50,** 1406 (1987).
11. P. M. Alsing, V. Kovanis, A. Gavrielides, and T. Erneux, Phys. Rev. A **53,** 4429 (1996).
12. J. Mork, B. Tromborg, and J. Mark, IEEE J. Quantum Electron. **28,** 93 (1992).
13. M. San Miguel, Q. Feng, and J. V. Moloney, Phys. Rev. A **52,** 1728 (1995).